# Effect of magnetic anisotropy on the transverse planar Hall resistance of $Ga_{1-x}Mn_xAs$ films grown on vicinal GaAs substrates

W. L. Lim,[1,*] X. Liu,[1] K. Dziatkowski,[1,2] Z. Ge,[1] S. Shen,[1] J. K. Furdyna,[1] and M. Dobrowolska[1]
[1]*Department of Physics, University of Notre Dame, Notre Dame, Indiana 46556, USA*
[2]*Institute of Experimental Physics, Warsaw University, 00-681 Warsaw, Poland*
(Received 18 May 2006; published 7 July 2006)

A striking asymmetry is observed in magnetic field dependence of the Hall resistance $R_{xy}$ in ferromagnetic $Ga_{1-x}Mn_xAs$ epilayers grown on vicinal GaAs substrates, caused by the superposition of the planar Hall effect (PHE) and the anomalous Hall effect (AHE). The asymmetry is a direct manifestation of the effect of magnetocrystalline anisotropy in $Ga_{1-x}Mn_xAs$, that confines the magnetization **M** to a preferred crystal plane *rather than to the plane of the film*, resulting in a nonzero component of **M** normal to the sample plane in vicinal samples. The simultaneous contributions of AHE and PHE to the same measured quantity provides valuable physical insight into the relationship of the two effects. The asymmetry of the resistance $R_{xy}$ occurring in the PHE geometry in vicinal $Ga_{1-x}Mn_xAs$ layers also allows one to obtain *four* distinct zero-field resistance states that depend on the history of the experiment, making this effect of potential interest for building a unique *four-state* memory device.

DOI: 10.1103/PhysRevB.74.045303 PACS number(s): 75.50.Pp, 75.30.Gw, 75.47.−m, 75.70.−i

## I. INTRODUCTION

Various forms of magnetic anisotropy have recently been studied in III-Mn-V ferromagnetic semiconductors (e.g., $Ga_{1-x}Mn_xAs$), with the aim of understanding the basic magnetic properties of these materials, and ultimately of exploring the potential of magnetic anisotropy for spintronic applications.[1–3] Data on in-plane and perpendicular cubic and uniaxial anisotropy fields obtained by ferromagnetic resonance (FMR)[4,5] and by magneto-optical Kerr effect (MOKE)[6] have contributed to our understanding of the dependence of magnetic anisotropy on strain, temperature, and on the concentration of charge carriers in III-Mn-V materials.[7] The influence of strain on magnetocrystalline anisotropy in $Ga_{1-x}Mn_xAs$ has already been extensively discussed by several research groups.[4,8–10] The recent discovery of the giant planar Hall effect (PHE) in thin $Ga_{1-x}Mn_xAs$ thin films has further enabled the exploration not only of magnetocrystalline anisotropy itself, but also of the evolution of domain walls during the process of magnetization reversal.[11–15]

One of the central issues of magnetic anisotropy in thin ferromagnetic (FM) films is to understand the relative roles of shape and magnetocrystalline anisotropy. For example, in metal FM films, which are typically characterized by a high value of magnetization **M**, shape anisotropy confines the easy axis of magnetization to the layer plane, while magnetocrystalline anisotropy plays a lesser role. In $Ga_{1-x}Mn_xAs$ films grown on (001) GaAs substrates the easy axis is known to lie in the layer plane. While this is usually ascribed to the compressive in-plane strain on the $Ga_{1-x}Mn_xAs$ film, the fact that in this case the (001) plane coincides with the sample plane makes it difficult to disentangle the relative roles of the shape and crystalline effects in determining the orientation of the easy axis.

Films grown on vicinal (tilted) substrates provide an ideal opportunity to separate the contributions of shape and crystalline anisotropy, since in the vicinal geometry the principal crystal axes no longer lie in the sample plane. In particular, by studying a series of vicinally grown $Ga_{1-x}Mn_xAs$ films with progressing inclination of the crystallographic axes relative to the morphological plane of the layers allows us to disentangle the effects of shape and magnetocrystalline anisotropies, and to conclude that the orientation of the easy axis is determined by the latter. This situation manifests itself in the simultaneous contributions of the planar Hall effect and the anomalous Hall effect (AHE) to the measured Hall resistance $R_{xy}$. Here we should recall from experiments on nonvicinal samples that AHE refers to the Hall resistance $R_{xy}$ observed in the standard Hall geometry, i.e., when the magnetic field is applied normal to the plane of the Hall bar, and arises from the effect of magnetization on the scattering of charge carriers; while PHE is observed with the magnetic field applied in the plane of the sample, and is caused by changes in orientation of the in-plane magnetization. As already noted, in vicinal samples both effects—PHE and AHE—contribute to the measured value of $R_{xy}$, providing important insights into the mechanisms which determine the orientation of the easy axis within the FM film.

In this paper we will use measurements of the Hall resistance $R_{xy}$ obtained with the magnetic field applied in the layer plane at various angles relative to the current as a means of comparing the properties of in-plane magnetization in $Ga_{1-x}Mn_xAs$ epilayers grown on standard (001) and on vicinal [slightly tilted relative to (001)] GaAs substrates. We should note here that the PHE exists in this geometry regardless of the vicinal tilt. The anomalous Hall effect (AHE) contribution, on the other hand, arises only due to the presence of a small but finite projection of the magnetization normal to the sample surface, an effect that is induced by magnetocrystalline anisotropy forcing the magnetization **M** to lie along a preferred crystallographic plane rather than along the plane of the film. Thus the AHE contribution to $R_{xy}$ measured in the PHE geometry is only present in vicinally grown samples.

 

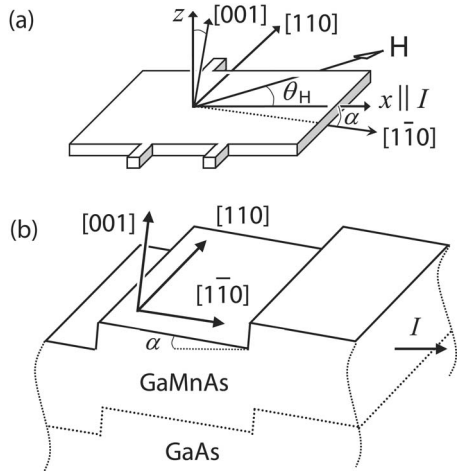


FIG. 1. Schematic diagram of (a) Hall bar orientations, also showing crystallographic directions and $x$ and $z$ axes; and (b) a $Ga_{1-x}Mn_xAs$ epilayer grown on a GaAs substrate with a vicinal angle $\alpha$ tilted away from [1$\bar{1}$0]. The atomic steps on the vicinal surface are exaggerated relative to the dimensions of the (001)-plane terraces.

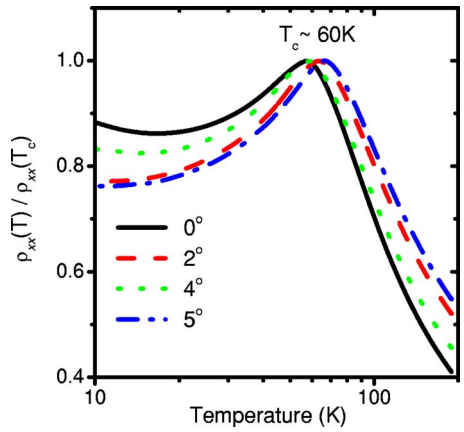


FIG. 2. (Color online) Normalized temperature dependence of resistivities at zero field for samples grown on substrates with vicinal angles 0°, 2°, 4°, and 5°.

## II. SAMPLE PREPARATION AND EXPERIMENTAL GEOMETRY

Specimens for this investigation were fabricated as follows. A 46 nm layer of $Ga_{1-x}Mn_xAs$ (with the Mn concentration fixed at $x \approx 0.07$) was grown on a standard semi-insulating (001) GaAs substrate and on three different vicinal substrates in a RIBER 32 R&D molecular beam epitaxy (MBE) system. The planes of the vicinal substrates were tilted by 2°, 4°, and 5° away from the (001) plane toward the (1$\bar{1}$1)B plane. During the $Ga_{1-x}Mn_xAs$ deposition the substrates with the different tilt angles were placed side by side on the same molybdenum block in order to ensure the same growth conditions. Due to the compressive strain resulting from lattice mismatch between $Ga_{1-x}Mn_xAs$ and the GaAs substrate,[16] all $Ga_{1-x}Mn_xAs$ samples produced in this growth had their easy axes in the (001) crystal plane.

It is relevant at this point to discuss the nature of strain induced by lattice mismatch in samples grown on substrates tilted relative to a principal crystallographic plane. Since in our case the vicinal angles are small (less or equal to 5° for all samples), the dimensions of the (001) terraces between the steps on the vicinal surface [see Fig. 1(b)] are large. Microscopically the growth on vicinal surfaces is thus still occurring on the (001) terraces, and the strain induced by the lattice mismatch during the growth of $Ga_{1-x}Mn_xAs$ layers is expected to remain fixed in the [001] direction. One therefore does not expect any significant differences between the nature (i.e., the crystallographic symmetry) of the strain in $Ga_{1-x}Mn_xAs$ grown on such terraces compared to that grown on a nontilted (001) substrate. In other words, in either case the direction of the easy axis in $Ga_{1-x}Mn_xAs$ induced by compressive uniaxial strain will be confined to the (001) plane, as is indeed observed in our experiments.

The samples described above were characterized by magnetotransport measurements using a five-probe Hall geometry with indium ohmic contacts. The epilayers were patterned into 50 $\mu$m $\times$ 250 $\mu$m Hall bars by photolithography, with the long axis oriented along the [1$\bar{1}$0] direction. The Hall bar geometry and the crystallographic profile of the vicinal $Ga_{1-x}Mn_xAs$ layers grown on the tilted substrates are shown in Figs. 1(a) and 1(b), respectively.

In discussing the magnetotransport measurements carried out on the vicinal layers, it is important to distinguish between the morphological sample plane (i.e., the measuring plane) and the (001) crystal plane. To make that distinction we will use the coordinates $x$, $y$, $z$ when referring to the macroscopic morphology of the layer, $z$ being the direction normal to the layer surface, $x$ the direction of the current flow, and $y$ the direction of the Hall voltage, as shown in Fig. 1. Magnetotransport discussed in this paper will involve the Hall resistance $R_{xy}$ measured in two field geometries: with field **H** applied in the plane of the sample (the $xy$ plane) at an arbitrary azimuthal angle, which for convenience we will continue to call the PHE geometry, even though in vicinal samples there is a (small but essential) AHE contribution in this configuration; and with **H** applied normal to the film ($\mathbf{H} \parallel z$), which we will refer to as the AHE geometry.

All $Ga_{1-x}Mn_xAs$ films used in this study exhibit ferromagnetism up to a transition temperature $T_c \sim 60$ °C, as indicated by the normalized resistivity peaks in Fig. 2. Since the ferromagnetic parameters of III-Mn-V systems, including the values of $T_c$, depend strongly on the carrier concentration,[2] the similarity of the $T_c$ values in all samples indicates that their carrier concentrations are also very close, estimated to be $p \sim (3.6 \pm 1.3) \times 10^{19}$ cm$^{-3}$ from Hall measurements carried out at 280 K. The $Ga_{1-x}Mn_xAs$ epilayers grown on substrates with 0°, 2°, 4°, and 5° vicinal angles will be labeled as samples *A*, *B*, *C*, and *D*, respectively. It is easily shown that for vicinal samples the distance between successive atomic steps on the surface [see Fig. 1(b)] is given by $l = (a/2)\cot(\alpha)$, where $a$ is the lattice constant of the material and $\alpha$ is the vicinal angle, i.e., the angle between the sample plane and the (001) crystallographic plane. Thus for samples *B*, *C*, and *D*, $l$=81 Å, 40 Å, and 32 Å, respectively.

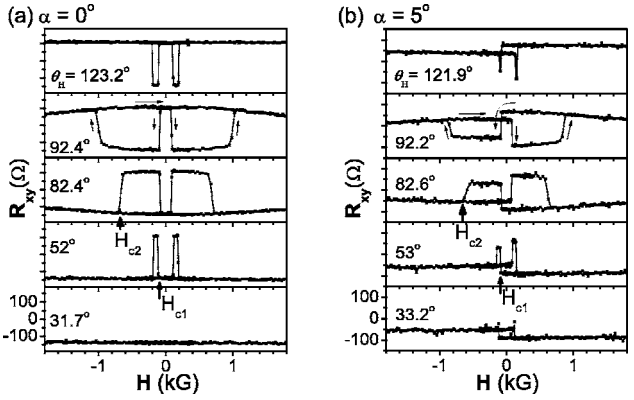


FIG. 3. Hall resistances $R_{xy}$ measured in the PHE geometry for $Ga_{1-x}Mn_xAs$ grown on (a) normal and (b) 5° vicinal substrate at different applied field angles $\theta_H$.

## III. EXPERIMENTAL RESULTS AND DISCUSSION

Figure 3 shows the Hall resistance $R_{xy}$ measured in the PHE geometry (field **H** in the $xy$ plane) on samples $A$ and $D$, performed at 4.2 K with applied magnetic field at various angles $\theta_H$ relative to the current $I$. The field was swept between +10 kG and −10 kG, a +10 kG field being applied prior to each field scan to saturate the magnetization of the $Ga_{1-x}Mn_xAs$ layer. In both Figs. 3(a) and 3(b) the value of $R_{xy}$ displays a two-step behavior during the field sweep,[11] well known in $Ga_{1-x}Mn_xAs$ epilayers with equivalent easy axes along the [100] and [010] directions, and with the in-plane hard axes along [110] and $[1\bar{1}0]$. We observe a striking difference between the behavior of $R_{xy}$ in samples $A$ and $D$. Specifically, the values of the Hall resistance plateaus (which correspond to the intermediate magnetization states in the process of magnetization reversal) are conspicuously unequal in sample $D$, although the magnitudes of the low-field vertical jumps in $R_{xy}$ are independent of the field angle, just as they are in sample $A$. One can see that there can be *four* distinct resistance states at $H \sim 0$ G, *depending on the history of the applied fields* (i.e., on the sequence of field strengths applied at a given angle). Before we proceed further, it should be noted that (i) the first jump of PHE for each $\theta_H$ occurs at almost the same field positions $H_{c1} \sim 100$ G in both samples $A$ and $D$; and (ii) the second jump—although its position is strongly angle-dependent—also occurs at similar fields $H_{c2}$ in both samples. These observations suggest that the in-plane anisotropy of sample $D$ is close to that of sample $A$. Similar behavior was also found in the other two tilted samples, indicating that these properties of $R_{xy}$ measured in the PHE geometry are general.

### A. Asymmetry of the planar Hall effect in vicinal $Ga_{1-x}Mn_xAs$ layers

We now turn to the unusual asymmetry observed in the magnitude of $R_{xy}$ in vicinal samples. We illustrate this in Fig. 4 by $R_{xy}$ data observed in the PHE geometry on sample $D$ at $\theta_H$=172°, which allows us to follow the evolution of the magnetization reversal in detail. In discussing the effect we will assume that the sample can be described by a single

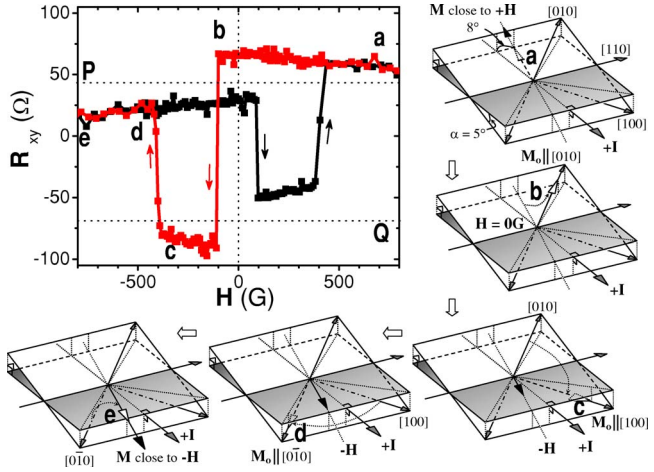


FIG. 4. (Color online) Low field Hall resistances $R_{xy}$ measured in the PHE geometry on $Ga_{1-x}Mn_xAs$ grown on 5° vicinal substrate at $\theta_H$=172°; and the schematic magnetization reversal evolution diagrams corresponding to the states from **a** to **e**. The shaded areas in the diagrams represent the sample plane (i.e., the plane containing the current and the applied magnetic field), and the unshaded areas correspond to the (001) crystal plane.

domain governed by the Stoner-Wohlfarth model.[17] This assumption is supported by the sharpness of the magnetic transitions seen in the figure. The geometry of the experiment is shown schematically by the successive diagrams next to the main figure, where shaded regions in the diagrams represent the sample plane (i.e., the plane containing the current and the applied magnetic field), and the white regions correspond to the (001) crystal plane. An initial positive 10 kG field was applied at the field angle $\theta_H$. Ideally, one would expect the saturated magnetization to lie in the sample plane if the applied field is strong enough to overcome the magnetocrystalline anisotropy energy.[18]

To understand the asymmetric behavior at low field, we first follow the succession of jumps in $R_{xy}$ that occurs during the process of magnetization reversal as the applied field is swept downward from +10 kG and then reversed. Upon reducing the field toward zero (e.g., going from **a** to **b** in Fig. 4), the magnetization gradually relaxes from its alignment with the field into a state where **M** is aligned along the easy axis [010], as depicted in schematic **b** on the right-hand side of Fig. 4. This state persists as the field is swept past zero to low negative field, and corresponds to the plateau marked **b**. Increasing the (negative) field further (to ca. −100 G) causes the magnetization jump into another intermediate magnetization state, with **M** aligned along the equivalent [100] easy axis via a 90° domain wall displacement. This corresponds to the jump of $R_{xy}$ from +66 Ω to −90 Ω seen in Fig. 4. The magnetization persists in this orientation (corresponding to plateau marked **c**) until the field reaches ca. −400 G in Fig. 4, at which the magnetization vector switches from its [100] orientation to $[0\bar{1}0]$, manifesting itself in the second jump in $R_{xy}$ (from −85 Ω to +20 Ω in Fig. 4) to the state depicted by schematic **d** below the figure. As the applied field continues to increase further in the negative direction, it will eventually turn the magnetization **M** toward the direction of the field

and bring it to saturation (depicted by schematic **e**).

The jumps in $R_{xy}$ discussed above are characteristic of PHE generally, i.e., they occur in vicinal as well as in nonvicinal samples, as illustrated by Figs. 3(b) and 3(a), respectively. However, in samples grown on nontilted substrate the jumps in $R_{xy}$ measured in the PHE geometry take place between *two* values, seen in Fig. 3(a). These values are represented by the dotted horizontal lines **P** and **Q** in Fig. 4. In vicinal samples, on the other hand, the plateaus in $R_{xy}$ observed in the PHE geometry are conspicuously asymmetric, as seen in Fig. 4.

To explain this asymmetry, it is of key importance to note that when **M** is confined by magnetocrystalline anisotropy to one of the easy axes ([100] or [010]) in the (001) plane, in vicinal samples there will exist a nonzero component of magnetization $M_z$ normal to the sample plane. The *sign* of $M_z$ determines the *sign* of the AHE contribution to $R_{xy}$. Consider for specificity the plateau observed during the sweep from +10 kG down (**a**→**b**; red curve). Just before the jump from plateau **b** to **c** the magnetization **M** is aligned along [010], and the projection of $M_z$ is pointing in the positive $z$ direction. In this case the AHE contribution *adds* to the planar Hall component raising the resultant value of $R_{xy}$ above the dotted horizontal line **P** corresponding to the PHE signal in a nonvicinal sample. After the jump from **b** to **c** the magnetization switches to the [100] direction. This reverses the sign of $M_z$, and thus also of the AHE contribution to $R_{xy}$, so that in the **c** plateau $R_{xy}$ is *below* the dotted line **Q** corresponding to a nonvicinal sample. As the negative magnetic field continues to increase, the second magnetization jump (between **c** and **d**) is to the $\mathbf{M}\|[0\bar{1}0]$ orientation. Note that after this switch $M_z$ remains negative, so that the AHE contribution to the measured $R_{xy}$ remains below the dotted line **P** in Fig. 4 that corresponds to $R_{xy}$ in a nonvicinal sample. By following the details of Fig. 4 one can see that during a complete sweep cycle (i.e., from +10 kG to −10 kG and back to +10 kG) the magnetization **M** describes a complete (clockwise) rotation: i.e., in the downward sweep process (from +10 kG to−10 kG; red curve) the sequence of jumps involves $[010]\rightarrow[100]\rightarrow[0\bar{1}0]$, while for the upward field sweep (from −10 kG to +10 kG; black curve) the sequence of magnetization orientations is along the path $[0\bar{1}0]\rightarrow[\bar{1}00]\rightarrow[010]$.

### B. Relationship of the planar and anomalous Hall effects

For completeness (since the AHE contribution plays a central role in the $R_{xy}$ asymmetry discussed in this paper), we also performed the $R_{xy}$ measurements in the AHE geometry on the vicinal samples, i.e., with the field applied perpendicular to the layer plane. One should recall here that in general the magnetic field dependence of the AHE signal observed on ferromagnetic films shows a hysteresis around $\mathbf{H}=0$ only for layers where **M** is normal to the layer plane. Figures 5(a)–5(c) show the $R_{xy}$ signal measured in the AHE geometry on samples *A*, *B*, and *D*. Here, we see clearly the gradual emergence and increase of the hysteresis around $\mathbf{H}=0$ for samples with increasing vicinal angle, clearly indicating the presence of a perpendicular component of **M** that increases with the vicinal angle $\alpha$.

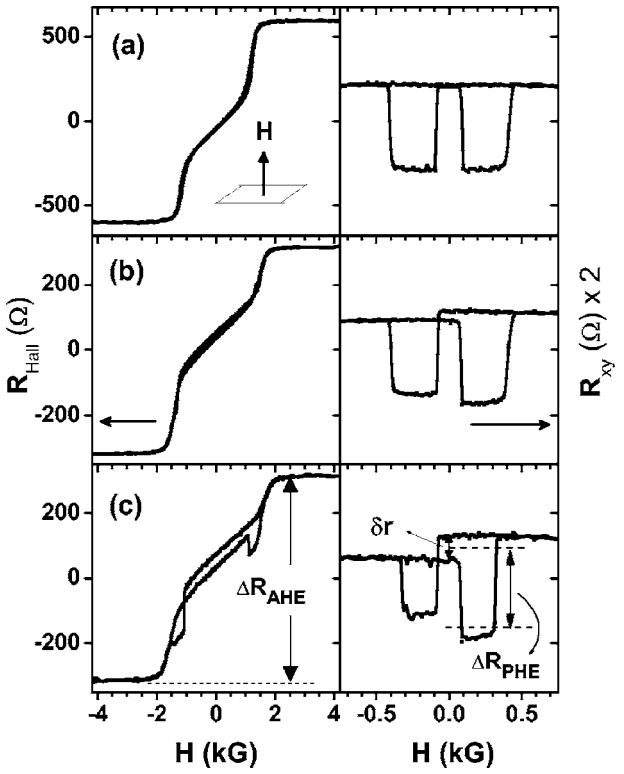


FIG. 5. Hall resistances $R_{xy}$ observed in AHE (left-hand panel) and PHE (right-hand panel, at $\theta_H=102°$) geometries for samples grown on vicinal substrates with (a) $\alpha=0°$, (b) 2°, and (c) 5° vicinal angles.

The value of $R_{xy}$ measured in the AHE geometry is expected to saturate when the field is sufficiently strong to turn the full magnetization of the sample **M** normal to the layer plane. In our samples this occurs above ~2.0 kG, as seen from the saturation of $R_{xy}$ in Fig. 5 (left-hand panels). Since the value of $R_{xy}$ at saturation (which we will indicate by $\Delta R_{\mathrm{PHE}}$, as shown in Fig. 5) is caused by the full magnetization $M_{\mathrm{sat}}$, and the asymmetric shift of $R_{xy}$ observed in the PHE geometry at $H\sim 0$ in vicinal samples (indicated by $\delta r$ in the figure) results from the AHE contribution caused by the projection $M_z$, we have $M_z/M_{\mathrm{sat}}=\delta r/\Delta R_{\mathrm{AHE}}$. Furthermore, when **M** at low fields is along one of the easy axes in the (001) plane, its projection normal to the sample plane is given by

$$\frac{M_z}{M_{\mathrm{sat}}}=\cos\frac{\pi}{4}\sin\alpha=\frac{\delta r}{\Delta R_{\mathrm{AHE}}}, \tag{1}$$

where $\alpha$ is the tilt angle of the vicinal plane with respect to (001). The factor $\cos\frac{\pi}{4}$ arise because the easy axis of **M** is along either the [100] or the [010] direction, and the tilt angle of the plane is in the $(1\bar{1}0)$ plane.

In Fig. 6(a) we plot $\delta r/\Delta R_{\mathrm{AHE}}$ for the vicinal angles 0°, 2°, 4°, and 5°. The striking agreement of the data with Eq. (1) provides compelling evidence that at low fields the magnetization **M** is confined to one of the easy axes in the (001)

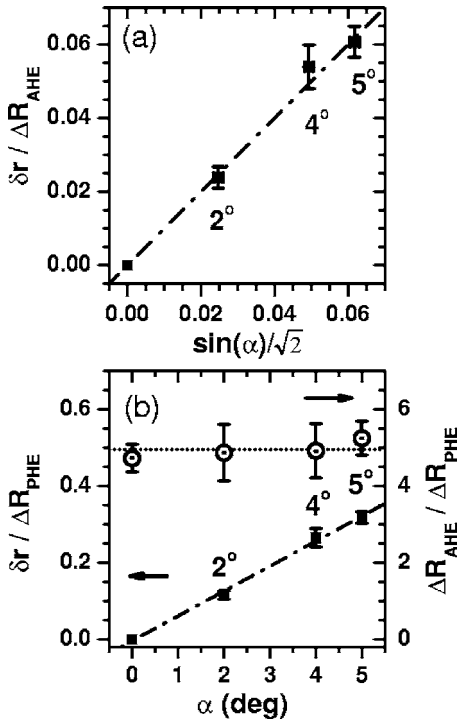


FIG. 6. Vicinal angular dependences of (a) the ratio $\delta r/\Delta R_{\mathrm{AHE}}$; and (b) $\delta r/\Delta R_{\mathrm{PHE}}$ (squares), suggesting a linear relationship between $\Delta R_{\mathrm{AHE}}$ and $\Delta R_{\mathrm{PHE}}$. The ratio $\Delta R_{\mathrm{AHE}}/\Delta R_{\mathrm{PHE}}$ is also shown (open circles). The dotted and dashed lines are guides for the eye.

crystal plane (presumably by the well established uniaxial magnetic anisotropy in thin $Ga_{1-x}Mn_xAs$ films[19–21]), which in vicinal samples results in a nonzero component $M_z$ normal to the sample plane.

Our analysis of the asymmetric shift $\delta r$ in $R_{xy}$ measured in the PHE geometry indicates that the ratio of $\delta r$ to the average jump in $R_{xy}$ denoted as $\Delta R_{\mathrm{PHE}}$ in the right-hand panel of Fig. 5(c) also increases linearly with the vicinal angle $\alpha$. The reader will recall that $\Delta R_{\mathrm{PHE}}$ corresponds to the distance between the horizontal lines **P** and **Q** in Fig. 4, and represents the true PHE in the samples, i.e., the jump in $R_{xy}$ *without* the AHE contribution. This relation is shown by the dashed-dotted plot of in $\delta r/\Delta R_{\mathrm{PHE}}$ in Fig. 6. The simultaneous observation that $\delta r/\Delta R_{\mathrm{AHE}}$ [Fig. 6(a)] and $\delta r/\Delta R_{\mathrm{PHE}}$ [Fig. 6(b)] vary linearly with $\alpha$ suggests that there exists a relationship between $\Delta R_{\mathrm{AHE}}$ and $\Delta R_{\mathrm{PHE}}$. Indeed, the analysis of our data yields $\Delta R_{\mathrm{AHE}}=c\Delta R_{\mathrm{PHE}}$, where $c=4.9\pm0.8$ is a proportionality constant *that is independent* of the applied fields, field angles, and of the vicinal angles. This result is somewhat unexpected, because AHE is conventionally formulated in term of skew or side-jump scattering of carriers that lead to a Hall voltage, while the giant PHE jumps are interpreted as resulting from anisotropic magnetoresistance (AMR) in the presence of strong spin-orbit coupling in ferromagnetic $Ga_{1-x}Mn_xAs$ samples.[11] We should note that the observation of this unexpected relationship is made possible because both effects—AHE and PHE—can be observed simultaneously in the same sample, where they are both *tied* by the same parameter $\delta r$ and can thus be compared under identical condition. While the observation of the relationship of AHE and PHE is at this point a phenomenological by-product of this investigation, it may shed valuable light on the underlying physics of both effects. It is reasonable to expect that the constant $c$ connecting the two effects depends on the hole and Mn concentrations. It would therefore be interesting to extend these measurements to samples with other values of these parameters in order to shed further light on this result.

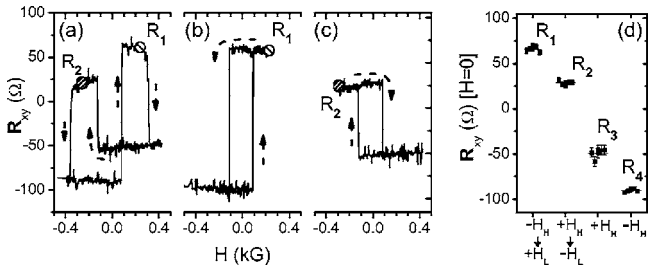


FIG. 7. Resistances $R_{xy}$ observed in the PHE geometry at $\theta_H=190°$ for a complete field sweeping loop from (a) −2.0 kG → +2.0 kG → −2.0 kG; (b) −2.0 kG → +0.2 kG → −2.0 kG; and (c) +2.0 kG → −0.2 kG → +2.0 kG. (d) Demonstration of nonvolatile memory states at $\theta_H=190°$ for the four values of $R_{xy}$ ($R_1=+66\ \Omega$, $R_2=+29\ \Omega$, $R_3=-49\ \Omega$ and $R_4=-90\ \Omega$) obtained by applying $H_H$(2.0 kG) and $H_L$(0.2 kG) in the PHE geometry in specific sequences before switching off the field.

In addition to its fundamental meaning, the fact that $\Delta R_{\mathrm{AHE}}/\Delta R_{\mathrm{PHE}}$ is a constant (see Fig. 6) also provides compelling support for the single-domain assumption which we use in interpreting our results. This can be argued as follows. The value of $\Delta R_{\mathrm{AHE}}$ is obtained from the saturation region of the AHE indicated in Fig. 5, i.e., when the magnetic field is strong enough to align all the magnetic moments normal to the sample plane, so that the sample is a single domain. The fact that the ratio $\Delta R_{\mathrm{AHE}}/\Delta R_{\mathrm{PHE}}$ is a constant then indicates that the measured contribution to PHE is also made by the entire (i.e., single) domain. The same conclusion can be drawn from the linearity of $\delta r/\Delta R_{\mathrm{AHE}}$. This is not at all surprising, since in $Ga_{1-x}Mn_xAs/GaAs$ specimens the domains are typically quite large.[12]

### C. Vicinal $Ga_{1-x}Mn_xAs$ layers as a four-valued memory structure

The above results clearly demonstrate that in $Ga_{1-x}Mn_xAs$ films it is the magnetocrystalline anisotropy rather than shape anisotropy that establishes the preferred direction along which the magnetization **M** tends to align. In addition to this conclusion, the observations reported in this paper also point to the possibility of a four-state magnetic memory device which can be operated by applying a specific sequence of magnetic fields to a vicinal sample. We demonstrate the idea of such a device using sample *D*. As shown in Fig. 7, using two field strengths, $H_H=2$ kG and $H_L=0.2$ kG applied at $\theta_H=190°$, it is possible to retain any of four different resistance states $R_{xy}$ at $H=0$, depending on the sequence in which these fields are applied before the field is switched off. For example, applying a *positive* $H_H$ and switching it off results in $R_{xy}=-49\ \Omega$; applying a negative $H_H$ gives $R_{xy}=-90\ \Omega$ after the field is switched off; applying

a sequence of $-H_H$ followed by $+H_L$ and then switching off the field results in $R_{xy}=+66\ \Omega$; and the field sequence $+H_H$, $-H_L$ results in $R_{xy}=+29\ \Omega$ after the field is switched off, as summarized in Fig. 7(d).

Although for a given sample the values of the four resistance states $R_{xy}$ illustrated in Fig. 7 do not depend on the azimuthal angle of the applied field $\theta_H$, the angle $\theta_H$ does determine the sequence of the fields required to obtain any of these states at zero field. Since the resistance states can be reversed upon crossing the hard axis, it is then possible to use two in-plane orthogonal fields as two logic inputs to set the actual field angle in any half-quadrant between the easy axes [100] and [010]. This will rearrange the sequential field operations required for reaching each of the resistance states. Such controls could resemble a magneto-logic device,[22] or a reconfigurable nonvolatile four-state magnetoresistance random access memory (MRAM) with double capacity as well as additional degrees for manipulation.

## IV. CONCLUDING REMARKS

We have successfully grown a series of 46 nm $Ga_{0.93}Mn_{0.07}As$ epilayers on tilted GaAs substrates with vicinal angles as high as 5°. Measurements in the PHE and AHE geometries on the vicinal samples reveal that the orientation of the easy axis of magnetization in $Ga_{1-x}Mn_xAs$ films does not originate from the shape of the specimen (shape anisotropy), magnetocrystalline anisotropy being the dominant mechanism which determines the direction of the easy axis. The Hall resistance $R_{xy}$ measured in vicinal samples in the PHE geometry shows a characteristic asymmetry as a function of the applied field, that contrasts sharply with $R_{xy}$ measured in the same geometry in nonvicinal $Ga_{1-x}Mn_xAs$ films. We have demonstrated that the above asymmetry arises from a contribution of the AHE caused by a small but finite component of magnetization **M** normal to the surface of the sample, because **M** is constrained to the easy axis (usually along the [100] or [010] direction) that in vicinal samples is not coincident with the layer plane.

The behavior of the asymmetry reported in this paper is especially interesting in that in samples with finite vicinal angle the values of $R_{xy}$ observed in the PHE geometry show *four* residual resistance states that depend on the history of how the field was applied before it was switched off, instead of the two states observed in PHE in nontilted samples. Using the above fourfold "memory" present in the Hall resistance $R_{xy}$, we were able to demonstrate a four-state MRAM memory device achieved by applying two magnetic fields in different sequences before the field is switched off.

The ability to investigate effects of PHE and AHE contributing simultaneously to the same effect in a series of samples provided the opportunity to discover that the two effects are related by a constant ratio, that is independent of the vicinal angle and field orientation. The fact that the same ratio applies to all samples in the series is quite surprising, because AHE is generally ascribed to processes different from those determining PHE (AHE is usually discussed in terms of skew or side-jump scattering of carriers; while PHE in $Ga_{1-x}Mn_xAs$ is described in terms of AMR). Although we do not understand the close relationship of PHE and AHE reported in this paper, this observation points to the possibility that the two effects are fundamentally related. We therefore feel that this observation provides important input into the picture of magnetotransport in ferromagnetic semiconductors.

We note that at low temperatures (ca. 4.2 K) in all our $Ga_{1-x}Mn_xAs$ samples, the easy axis of magnetization is along the crystallographically equivalent [100] and [010] directions in the (001) plane, consistent with the observations reported by Welp *et al.*[19] However, it is well known that the easy axis can change from [100] or [010] to the [110] orientation as the temperature is increased;[12,23] additionally, under certain conditions the easy axis can even switch from the in-plane to an out-of-plane orientation with changing temperature.[24] We have indeed observed interesting changes in the behavior of $R_{xy}$ in our vicinal $Ga_{1-x}Mn_xAs$ samples at higher temperatures (ca. 30 K and above; not shown), that we ascribe to the former (in-plane) switching of the easy axis. A detailed discussion of these effects is outside the scope of the present paper, and will be presented elsewhere.[25] In case of the latter possibility (i.e., the temperature-induced in-plane to out-of-plane rotation of the easy axis), when this happens in vicinal samples, the value of the out-of-plane magnetization is expected to increase rapidly, until eventually it lies along the [001] direction (but not along the normal to the plane *xy*). In this situation, the roles of PHE and AHE in $R_{xy}$ are expected to reverse, PHE becoming a perturbation to AHE, similar to the results presented by Liu *et al.*[26] We should note that before that happens, there will occur an *intermediate* region where AHE and PHE are equal or comparable. In this situation the asymmetry of $R_{xy}$ is expected to be particularly pronounced. We therefore feel that exploring vicinal samples under conditions where varying the temperature changes the orientation of the easy axis from in-plane to out-of-plane should be especially informative, shedding valuable additional light on AMR, PHE, and AHE in $Ga_{1-x}Mn_xAs$, and on the temperature dependence of magnetic anisotropy in this material.

## ACKNOWLEDGMENTS

This work was supported by the NSF Grant No. DMR02-45227 and NSF-NIRT Grant No. DMR02-10519.

*Electronic address: wlim@nd.edu

[1] S. A. Wolf, D. D. Awschalom, R. A. Buhrman, J. M. Daughton, S. von Molnar, M. L. Roukes, A. Y. Chtchelkanova, and D. M. Treger, Science **294**, 1488 (2001).
[2] T. Dietl, H. Ohno, F. Matsukura, J. Cibert, and D. Ferrand, Science **287**, 1019 (2000).
[3] H. Ohno, Science **291**, 840 (2001).
[4] X. Liu, Y. Sasaki, and J. K. Furdyna, Phys. Rev. B **67**, 205204 (2003).
[5] K. Dziatkowski, M. Palczewska, T. Slupinski, and A. Twardowski, Phys. Rev. B **70**, 115202 (2004).
[6] G. P. Moore, J. Ferre, A. Mougin, M. Moreno, and L. Daweritz, J. Appl. Phys. **94**, 4530 (2003).
[7] J. K. Furdyna, X. Liu, T. Wojtowicz, W. L. Lim, U. Welp, and V. K. Vlasko-Vlasov, in *Advances in Solid State Physics*, edited by K. Bernhard (Springer-Verlag, Berlin, 2004).
[8] T. Dietl, H. Ohno, and F. Matsukura, Phys. Rev. B **63**, 195205 (2001).
[9] M. Abolfath, T. Jungwirth, J. Brum, and A. H. MacDonald, Phys. Rev. B **63**, 054418 (2001).
[10] S. C. Masmanidis, H. X. Tang, E. B. Myers, Mo Li, K. De Greve, G. Vermeulen, W. V. Roy, and M. L. Roukes, Phys. Rev. Lett. **95**, 187206 (2005).
[11] H. X. Tang, R. K. Kawakami, D. D. Awschalom, and M. L. Roukes, Phys. Rev. Lett. **90**, 107201 (2003).
[12] U. Welp, V. K. Vlasko-Vlasov, X. Liu, J. K. Furdyna, and T. Wojtowicz, Phys. Rev. Lett. **90**, 167206 (2003).
[13] K. Hamaya, T. Taniyama, Y. Kitamoto, R. Moriya, and H. Munekata, J. Appl. Phys. **94**, 7657 (2003).
[14] H. X. Tang, S. Masmanidis, R. K. Kawakami, D. D. Awschalom, and M. L. Roukes, Nature (London) **431**, 52 (2004).
[15] A. W. Holleitner, Appl. Phys. Lett. **85**, 5622 (2004).
[16] H. Ohno, J. Magn. Magn. Mater. **200**, 110 (1999).
[17] E. C. Stoner and E. P. Wohlfarth, Philos. Trans. R. Soc. London, Ser. A **240**, 74 (1948).
[18] However, at high fields, the planar Hall resistance is not flat, but continues to change gradually (as seen at point, **a** in Fig. 4). This suggests that at low field the magnetization **M** lies not in the sample plane, but presumably in a preferred crystalline plane, from which it is gradually dragged to the field direction as the field increases.
[19] U. Welp, V. K. Vlasko-Vlasov, A. Menzel, H. D. You, X. Liu, J. K. Furdyna, and T. Wojtowicz, Appl. Phys. Lett. **85**, 260 (2004).
[20] K. Hamaya, T. Taniyama, Y. Kitamoto, T. Fujii, and Y. Yamazaki, Phys. Rev. Lett. **94**, 147203 (2005).
[21] M. Sawicki, K.-Y. Wang, K. W. Edmonds, R. P. Campion, C. R. Staddon, N. R. S. Farley, C. T. Foxon, E. Papis, E. Kaminska, A. Piotrowska, T. Dietl, and B. L. Gallagher, Phys. Rev. B **71**, 121302(R) (2005).
[22] C. Pampuch, A. K. Das, A. Ney, L. Daweritz, R. Koch, and K. H. Ploog, Phys. Rev. Lett. **91**, 147203 (2003).
[23] K.-Y. Wang, M. Sawicki, K. W. Edmonds, R. P. Campion, S. Maat, C. T. Foxon, B. L. Gallagher, and T. Dietl, Phys. Rev. Lett. **95**, 217204 (2005).
[24] X. Liu and J. K. Furdyna, J. Phys.: Condens. Matter **18**, R245 (2006).
[25] W. L. Lim, Ph.D. thesis, University of Notre Dame.
[26] X. Liu, W. L. Lim, L. V. Titova, M. Dobrowolska, J. K. Furdyna, M. Kutrowski, and T. Wojtowicz, J. Appl. Phys. **98**, 63904 (2005).